

# Full scale flexural test of jointed concrete members strengthened with post-tension tendons with internal anchorage



Tatsuhiko Mimoto<sup>a,b</sup>, Isamu Yoshitake<sup>a,\*</sup>, Takuya Sakaki<sup>a</sup>, Takafumi Mihara<sup>b</sup>

<sup>a</sup> Department of Civil and Environmental Engineering, Yamaguchi University, 2-16-1 Tokiwadai, Ube, Yamaguchi 755-8611, Japan

<sup>b</sup> Kyokuto Kowa Corporation, Hikarimachi 2-6-31, Higashi-ku, Hiroshima, Hiroshima 732-0052, Japan

## ARTICLE INFO

### Article history:

Received 22 July 2016

Revised 15 September 2016

Accepted 19 September 2016

### Keywords:

Internal anchorage  
Strengthening  
Prestressing tendon  
Flexural test  
Water permeability  
Joint

## ABSTRACT

A new strengthening system, which embeds a post-tensioned PC bar tendon into the wedge-shaped anchorage of an existing concrete member, was developed. Previously, the adequate load-bearing capacity of the prestressing tendon anchorage was confirmed on simple element specimens. In the present study, the developed system is applied to the addition of new concrete members to old concrete structures. The strengthening effect of the system was examined in a loading test on jointed full-scale concrete members. The saltwater permeability at the joint was also examined. The flexural properties of the jointed members were compared to those of concrete beams jointed with conventional post-installed adhesive anchors. The concrete beams jointed by the proposed system exhibited superior crack-resistance and load-carrying capacity, and their joints were strongly water-impermeable.

© 2016 Elsevier Ltd. All rights reserved.

## 1. Introduction

As is well known, concrete materials are vulnerable to tensile forces and frequently crack under internal and external forces. Therefore, concrete structures are usually reinforced by post-tensioned prestressing systems. Owing to their effectiveness and reliability, prestressed concrete (PC) structures have become popularized around the world. In addition, technical papers and reports on post-tensioning techniques have been widely published. In recent years, conventional prestressed tendons have been supplemented by advanced materials such as fiber reinforced polymers (FRPs) [3,11,27,24,15,16,4,28,14,22]. Flexural tests on prestressed concrete using various prestressing-materials are often conducted for assessing the fundamental structural performance of reinforced concrete structures.

Ng and Tan [18] developed a simple “pseudo-section analysis” method for externally prestressed concrete beams subjected to flexure. In addition, Ng and Tan [19] examined the flexural behavior of the prestressed beams and confirmed applicability of the proposed analytical model. Park et al. [21] conducted flexural tests of post-tensioned girders using high-strength strands. The flexural behaviors of their girders well agreed with the predictions of current design codes, although the concrete crack widths and stresses in the reinforcements slightly exceeded the specified limits.

Akiyama et al. [1] examined the flexural behaviors of cylindrical concrete pile prestressed with unbonded bars. They found that the load capacity of prestressed concrete pile was greatly increased by confining the pile between carbon fiber (CF) sheets. Kim et al. [12] developed a post-tensioning method for near-surface mounted (NSM) carbon fiber reinforced polymer (CFRP) strips, and estimated the anchorage capacity in comparative finite element simulations. Vu et al. [25] proposed a structural model of post-tensioned prestressed beams with unbonded tendons. Their model accurately predicted the deformations observed in experimental flexural tests. The structural responses of post-tensioned concrete slab/wall structures have also been extensively reported [29,7,6,5,26,2,13,8].

The existing concrete members in civil infrastructures become deteriorated by aging, and require regular strengthening and/or upgrading. Prestressing tendons and cables are generally arranged outside of the existing concrete members, demanding adequate workspace for the strengthening work. Recently, the present authors developed a new strengthening system using a conventional post-tensioning PC tendon [17]. The prestressing system uses an internal anchorage within existing concrete members. The tendon can be firmly anchored in a wedge-shaped hole filled with high strength mortar. This post-tensioning system also enables the addition of new concrete members to existing concrete structures. Whereas conventional RC jointed members are vulnerable to steel corrosion at the joints of the new and old

\* Corresponding author.

E-mail address: [yositake@yamaguchi-u.ac.jp](mailto:yositake@yamaguchi-u.ac.jp) (I. Yoshitake).

concrete, the developed prestressing system may increase the durability of the jointed structure. To assess the applicability of the new system, the present studies examine concrete members joined by the developed post-tensioning method.

Previous investigations on jointed concrete members have evaluated the structural performance and durability of segmented element systems. Turmo et al. [20] predicted the structural behavior of segmental concrete elements joined by external pre-stressing in numerical simulations. The applicability of their model was confirmed in comparisons between their predictions and experimental observations. Pillai et al. [23] studied the service reliability of segmental PC bridges in corrosive environments. They proposed a method that predicts the time-variant service reliability index, accounting for damage to PC tendons and other uncertainties.

The present study examines the workability of the post-tensioning system in full-size concrete members, and confirms the improved structural performance and durability of structures reinforced by the system. Full-scale reinforced concrete (RC) beams were connected by the developed method, and subjected to flexural tests. The results were compared against those of RC beam specimen jointed with conventional post-installed adhesive anchors. To examine their water permeability and steel corrosion resistance, jointed concrete beams were also exposed to saltwater for 5 weeks. This paper reports the cracking resistance, load-bearing capacity and saltwater permeability of the strengthened beams.

## 2. Strengthening method using post-tension tendons with internal anchorages

The developed strengthening system requires conventional pre-stressing bars, high strength mortar and a wedge-shaped hole (Fig. 1) formed by a special drilling device (see Fig. 2(a)). The drilling process of the hole is described in Fig. 2(b). Fig. 3 schematizes the strengthening process of the developed system. The prestressing tendon is firmly anchored in the internal wedge hole filled with high-strength mortar. Further details of the post-installed anchorage system are described in Mimoto et al. [17].

As shown in Fig. 3, the developed system can add new concrete members to existing concrete structures. A typical application is widening the slab width of concrete bridges (see Fig. 4). Concrete joints formed by the post-installed prestressing method may be much more durable than conventional jointed RC structures.

## 3. Methodology

### 3.1. Materials and mixture proportion

Table 1 lists the materials used in the experimental investigation. The conventional reinforcing materials were those used in

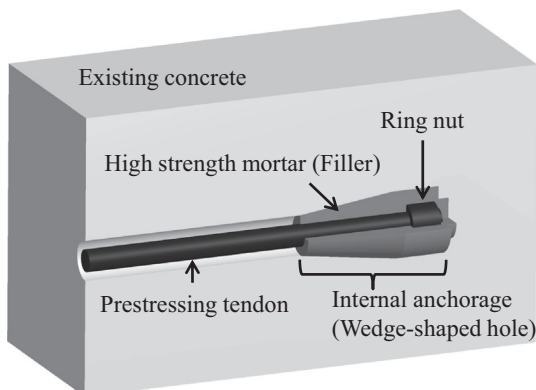
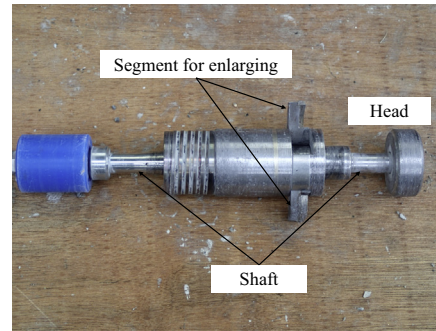
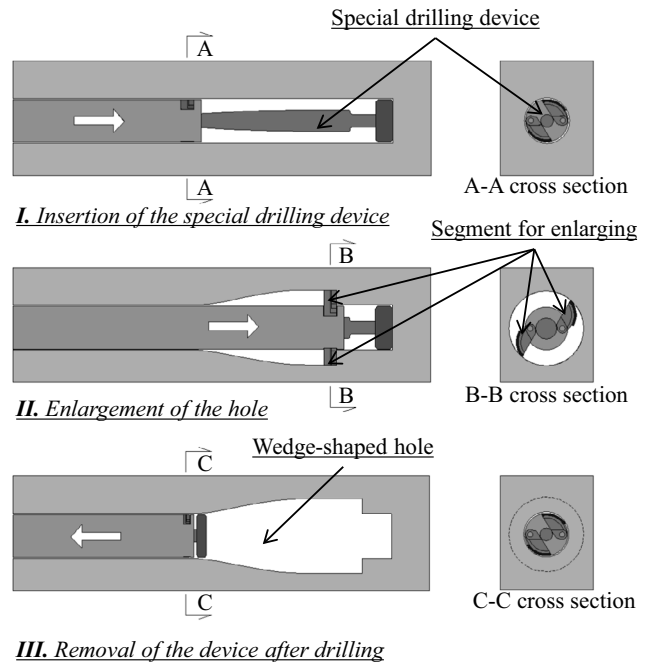


Fig. 1. Schematic of the internal anchorage system [17].



(a) Special drilling device



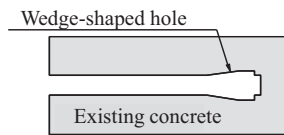
(b) Drilling process

Fig. 2. Drilling of the wedge-shaped hole in concrete [17]: (a) Special drilling device; (b) Drilling process.

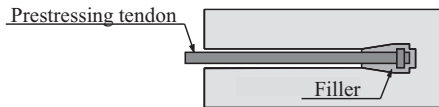
previous studies. The mixture proportions of the concrete and mortar are summarized in Table 2. The mixture of concrete (A) complies with that of general RC structures in Japan. The water-to-cement ratio was reduced in concrete (B) (relative to concrete (A)) to improve its strength and durability. The specified compressive strengths of concrete mixtures (A) and (B) are 24 MPa and 30 MPa, respectively. To ensure sufficient strength and the appropriate fresh properties, the wedge-shaped anchorage was filled with commercial mortar (premix type). According to the manufacture sheet, the minimum compressive strength of mortar is 100 MPa at the age of 28 days. Detailed information about the filling material cannot be described here because of a commercial contract with the manufacturer.

This study reports the mechanical properties (compressive strength, Young's modulus and Poisson's ratio) of the concretes and mortar. Consistent with the Japanese standard and the authors' previous study [17], each test was conducted on three cylindrical concrete specimens (100 mm diameter  $\times$  200 mm height) and three cylindrical mortar specimens (50 mm diameter  $\times$  100 mm height). The mechanical properties of the concretes and the high-strength mortar are summarized in Table 3.

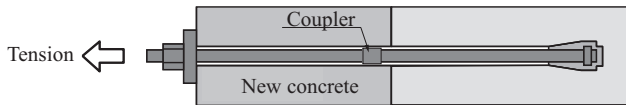
[Step 1] Concrete core drilling for internal anchorage (wedge-shaped hole)



[Step 2] Install of a prestressing tendon  
Fill high strength mortar into the wedge-shaped hole



[Step 3] Placing of new concrete (option)  
Provide tensile force (pull) to the prestressing tendon



[Step 4] Grouting

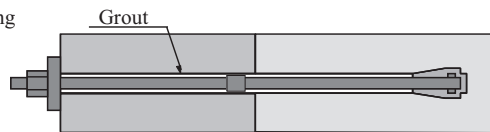


Fig. 3. Strengthening system process using a prestressing tendon fixed in the internal anchorage [17].

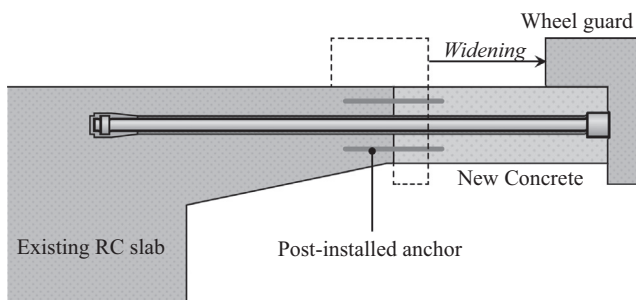


Fig. 4. Typical application of the proposed system (increasing the slab width of a concrete bridge).

### 3.2. Test specimens

The applicability of the developed post-tensioning system was examined on full-scale jointed concrete members. Fig. 5(a)–(d) shows schematics of the jointed beam specimens and the arrangement of the reinforcing bars. Each beam was 400 mm high, 800 mm deep and 3000 mm long. Specimen PC-0 is a control beam embedding tendons that are not post-tensioned. Specimen PC-1 is a jointed beam strengthened by the developed post-tensioning system. Both specimens were embedded with two prestressing tendons (each of 23 mm diameter). Two wedge-shaped holes were drilled in 10-day-old concrete (A) by a special device (Fig. 2a). Following Mimoto et al. [17], the diameter and length of the wedge-shaped hole was 66–42 mm and 100 mm, respectively. The water required for drilling was removed by a vacuum (340 W), and the hole size was confirmed by microscopy and a special measurement tool. The drilled hole was filled with high-strength mortar and inserted with the tip of the tendon. At age 38 days, the concrete (A) member embedding the tendon was conjoined with cast-in-place concrete (B). Fig. 6(a) presents the jointed concrete substrate

Table 1  
Materials used in the experimental study.

Concrete materials	Type	Density
Water (W)		1.00 g/cm <sup>3</sup>
Cement (C)	Ordinary Portland cement	3.16 g/cm <sup>3</sup>
Fine aggregate (S)	Crashed sand	2.64 g/cm <sup>3</sup>
Coarse aggregate (G)	Crashed stone	2.68 g/cm <sup>3</sup>
Admixture (AD)	Superplasticizer	1.04 g/cm <sup>3</sup>
Materials	Properties	
Reinforcing bar	JIS G-3112; Nominal diameter: 13 mm (D13) Yield strength: 345 MPa; Young's modulus: 206 GPa	
Post-installed bar	JIS G-3112; Nominal diameter: 16 mm (D16) Yield strength: 345 MPa; Young's modulus: 206 GPa	
Prestressing tendon	JIS G-3109; Nominal diameter: 23 mm; Type B-1 Tensile strength: 1080 MPa; Young's modulus: 202 GPa	
Ring nut	JIS G-3101; 38 mm diameter × 30 mm height Yield strength: 235 MPa; Young's modulus: 206 GPa	
Bearing plate with a hole	JIS G-3101; Dimensions: 120 × 120 × 25 mm Yield strength: 235 MPa; Young's modulus: 206 GPa	
Filling material	High-strength mortar (see Tables 2 and 3)	
Epoxy resin	Compressive strength: 104.2 MPa; Tensile strength: 20.7 MPa	

Table 2  
Mixture proportions of the concrete specimens.

Type	w/cm <sup>a</sup>	W	C	S	G	AD	Air
Conc. A	0.53	175 kg/m <sup>3</sup>	330 kg/m <sup>3</sup>	887 kg/m <sup>3</sup>	978 kg/m <sup>3</sup>	1.16 kg/m <sup>3</sup>	4.5%
Conc. B	0.50	169 kg/m <sup>3</sup>	338 kg/m <sup>3</sup>	874 kg/m <sup>3</sup>	1000 kg/m <sup>3</sup>	2.37 kg/m <sup>3</sup>	4.5%
Mortar <sup>b</sup>	0.12	1.2 kg/mix	10 kg/mix		N/A	N/A	N/A

<sup>a</sup> Water–cementitious material ratio.

<sup>b</sup> Premix mortar (filler).

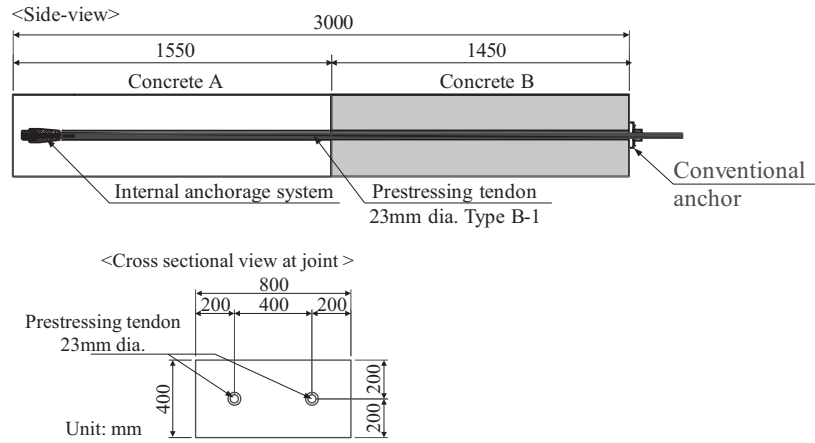
Table 3  
Properties of the materials used in the study.

	Concrete A	Concrete B	Mortar
Specified strength (MPa)	24	30	120
Production date	July-3, 2015	Aug.-10, 2015	July-13, 2015
Conc. slump/mortar flow (cm)	12.0	12.0	12.8 <sup>a</sup>
Compressive strength (MPa)	39.9	49.1	140.1
Young's modulus (GPa)	27.2	34.8	45.0
Poisson's ratio	0.17	0.18	0.22

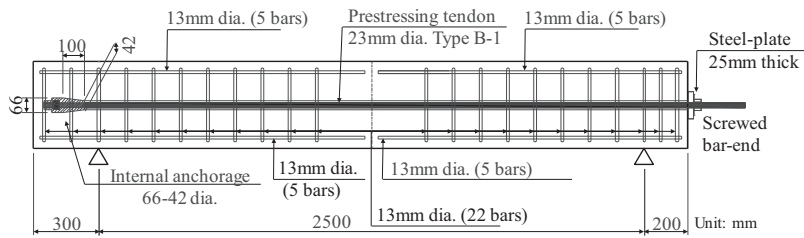
<sup>a</sup> Cylinder test (50 mm dia. × 100 mm height).

roughened by chipping with an impact hammer. After anchoring for 3 days, the tendon installed in specimen PC-1 was subjected to a tensile force of 320.8 kN. The axial force applied to each tendon (allowable load for design) was approximately 70% of the load-bearing capacity (448.7 kN) of the prestressing bar, as specified in Japanese industrial standards [10,17].

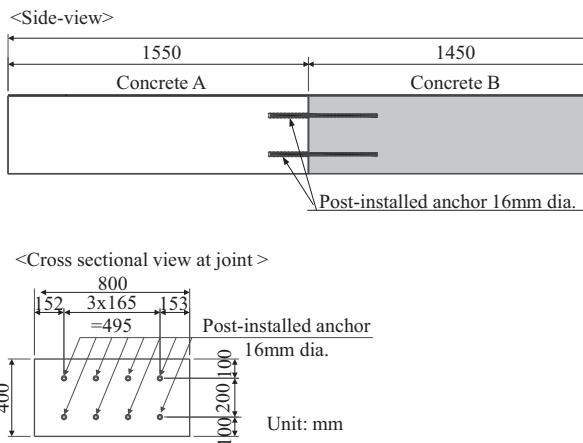
Specimen RC is a conventional jointed structure using post-installed adhesive anchors. In this specimen, eight reinforcing bars (each of 16 mm nominal diameter) were installed and bonded with epoxy resin (Table 1). Cast-in-place concrete (B) was added to the



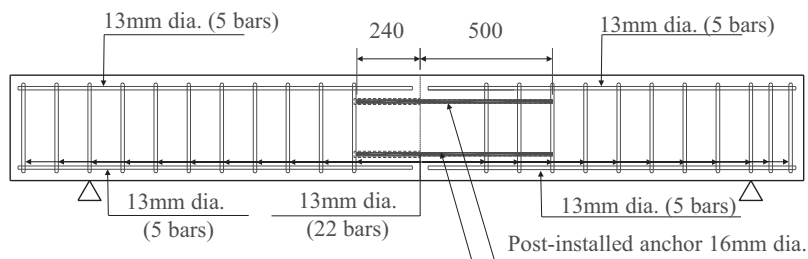
(a) Schematics of PC-0 and PC-1



(b) Rebars arrangement of PC-0 and PC-1



(c) Schematic of RC



(d) Rebars arrangement of RC

Fig. 5. Test specimens: (a) Schematics of PC-0 and PC-1; (b) Rebars arrangement of PC-0 and PC-1; (c) Schematic of RC; (d) Rebars arrangement of RC.

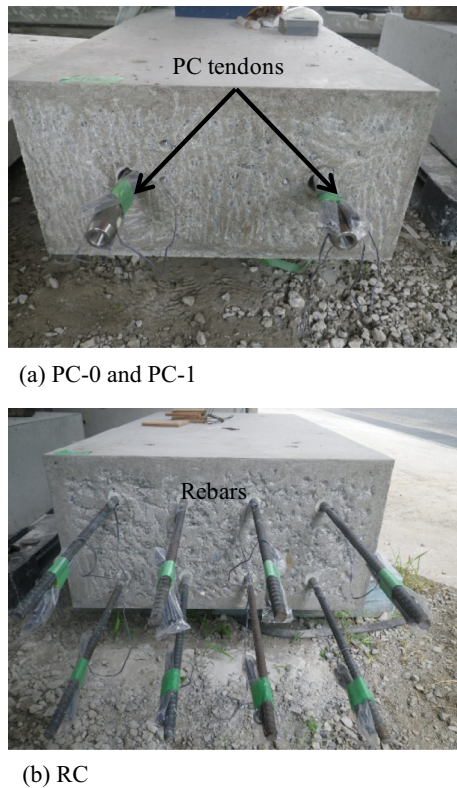


**Fig. 6.** Cross-sections of the concrete specimens at their joints: (a) PC-0 and PC-1; (b) RC.

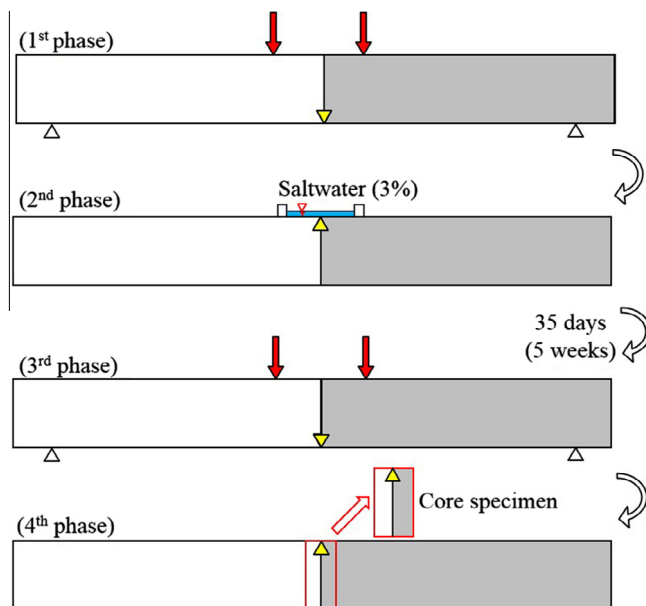


**Fig. 7.** Schematic of the test procedure.

concrete (A) of this specimen (see Fig. 6(b)) at the same time as specimens PC-0 and PC-1.

It should be noted that the reinforcement arrangements for these specimens were designed to achieve almost equal yielding load. The designed yielding loads are 188 kN for PC-1 and 186 kN for RC, respectively.

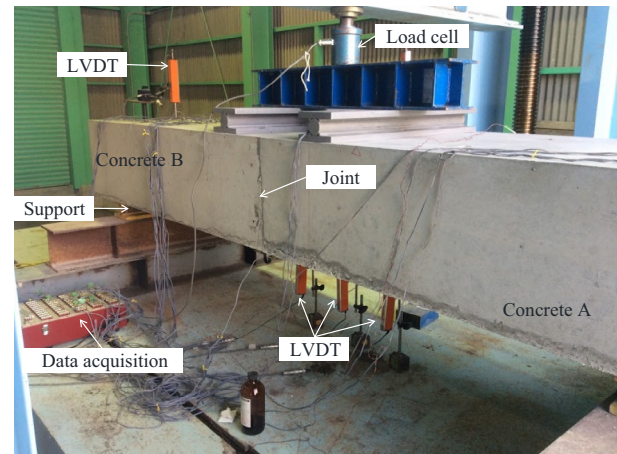


**Fig. 8.** Flexural test of full-scale jointed concrete beams.

### 3.3. Test procedure

Fig. 7 presents the test procedure of the experimental investigation. To ensure joint opening, the flexural test was first conducted on 28-day-old concrete (B). Hereafter, openings are referred to as *joint-cracks* for convenience. The load on specimen RC was increased until the crack width at the joint reached 0.2 mm, as specified in a Japanese guideline [9]. The observed maximum load in the first phase was then applied to specimens PC-0 and PC-1. In the second phase, the cracked beams were reversed and the concrete joints were exposed to saltwater (3%) for 35 days. In the third phase, the concrete joints were removed from the saltwater, and their load-carrying capacity was again determined in a flexural test. Finally, in the fourth phase, the chloride penetration depth was examined in concrete cores obtained from the joints of each specimen. The flexural and the salt-water permeability tests are described below.

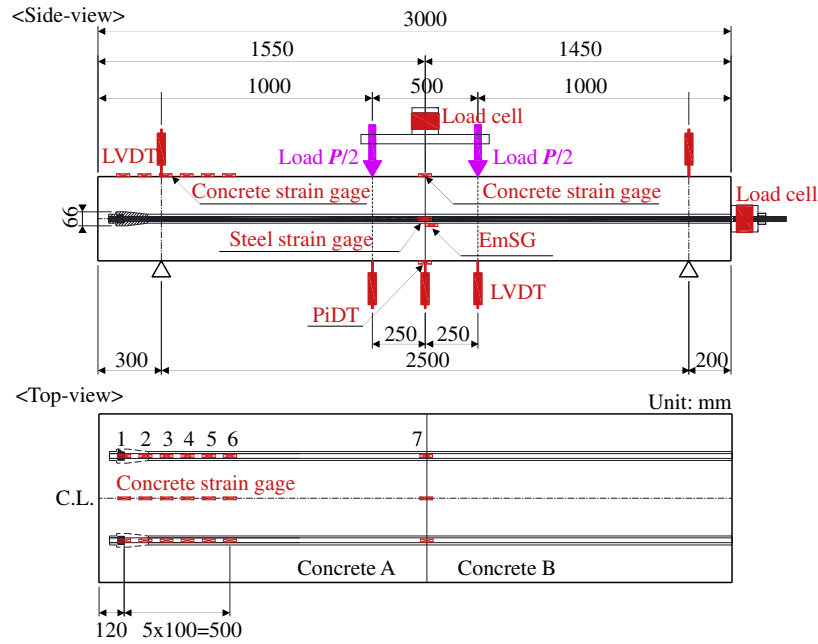
#### 3.3.1. Flexural test

Fig. 8 presents the flexural test conducted on the full-scale jointed concrete beams. The jointed beams were monotonically loaded in a four-point bending apparatus, and subjected to a flexural load applied by a hydraulic jack system. The beam span and loading span lengths were 2500 mm and 500 mm, respectively.

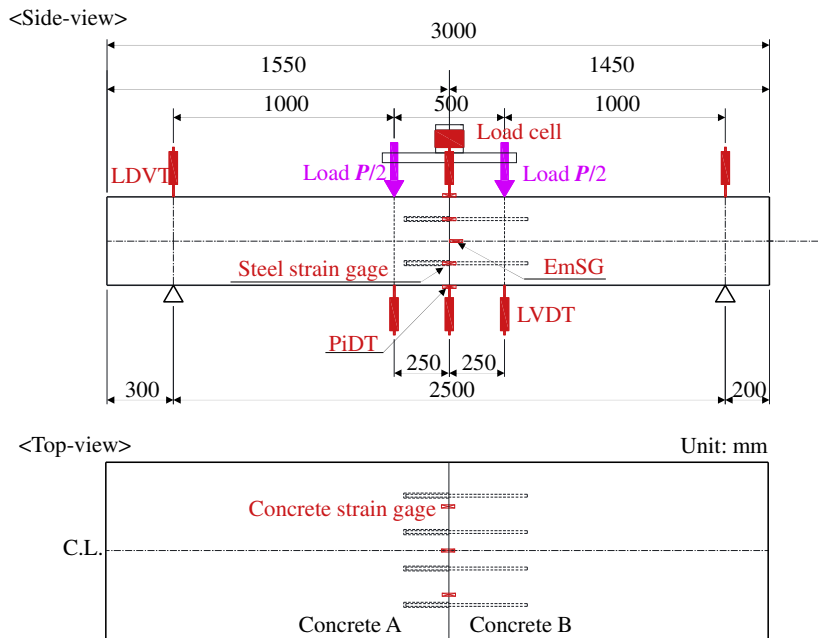
Fig. 9 illustrates the arrangement of the strain gages and related sensors. The concrete surfaces and reinforcing bars of the three specimens were affixed with wire strain gages of lengths 60 mm and 3 mm, respectively. The internal stress was observed by embedded-strain-gages (EmSGs) set into concrete (B), and the force on the prestressing bars of PC-1 was monitored by center-hole load cells. The deflection was monitored by linear variable displacement transducers (LVDTs) placed on the top and bottom surfaces of the beams. In addition, the joint crack width was observed by PI-shaped displacement transducers (PiDTs) placed on the bottoms of the joints. Table 4 lists the capacities and accuracies of the sensors used in the flexural test.

#### 3.3.2. Saltwater permeability test

Fig. 10 outlines the saltwater permeability test. The concrete joints of the concrete beams tested in the first phase were subjected to 3% salt water for 35 days (5 weeks). After the third phase, cylindrical specimens (diameter = 100 mm) were extracted from the concrete joints by a dry coring method. To check the improved durability of concrete strengthened with the post-tensioning system, the chloride penetration depths in the core specimens were examined by a silver nitrate spraying method.



(a) PC-0 and PC-1



(b) RC

Fig. 9. Arrangement of strain gauges, EmST, LVDTs and PiDTs: (a) PC-0 and PC-1; (b) RC.

Table 4  
Sensors used in the experimental tests.

Gages	Gage length	Resistance	Minimum measurement
For concrete	60 mm	120 Ω	$1.0 \times 10^{-6}$
For rebars	3 mm	120 Ω	$1.0 \times 10^{-6}$
EmST	60 mm	120 Ω	$1.0 \times 10^{-6}$
Sensors	Capacity	Rated output	Minimum measurement
LVDT	0–100 mm	2.5 mV/V	0.1 mm
PiDT	–2 mm – +2 mm	2.0 mV/V	0.001 mm
Load cells	Capacity	Rated output	Minimum measurement
	0–500 kN	1.5 mV/V	0.1 kN

## 4. Results and discussion

### 4.1. Crack resistance at the joint

The RC specimen developed its first joint crack under a load of 68.5 kN. After the cracking, the applied load was increased until the crack width reached 0.2 mm (at approximately 73 kN). The same load (73 kN) was then applied to specimens PC-0 and PC-1. After measuring the crack widths by the PiDTs, the 73 kN load was immediately removed. Residual cracks were also observed. The maximum loads and crack widths are summarized in Table 5, and the crack widths and upper surface strains on the concrete are



**Fig. 10.** Saltwater permeability test: (a) Concrete joint subjected to saltwater; (b) Test condition (35 days); (c) Dimensions of the test specimens; (d) Dry coring; (e) Core specimens.

**Table 5**  
Load and cracks observed in the first phase of the experimental procedure.

	RC	PC-0	PC-1
Load (kN)	72.7 <sup>a</sup>	73.0 <sup>a</sup>	73.4 <sup>a</sup>
Max. crack width (mm)	0.216	0.013	0.008
Residual crack width (mm)	0.085	0.003	0.001

<sup>a</sup> Load at the crack width of approximately 0.2 mm in the specimen RC.

presented in panels (a) and (b) of Fig. 11, respectively. The initial strain of specimen PC-1 is the prestress strain measured by the EmSG (Fig. 11(b)). The maximum and residual crack widths and strains were significantly smaller in specimen PC-1 than in specimen RC. Interestingly, specimen PC-0 (like the prestressed specimen PC-1) responded almost linearly to the load.

#### 4.2. Load bearing capacity and deformation

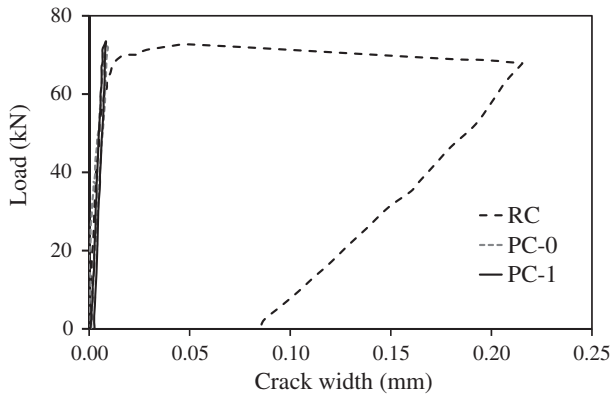
The load–midspan deflection responses and the maximum load and deflections are presented in Fig. 12(a) and Table 6, respec-

tively. During this flexural test, the load was increased until the deflection reached 5 mm. This deflection limit ensures the safety of the loading test on the prestressed concrete member (PC-1). Thereafter, the load was gradually removed to monitor the residual properties.

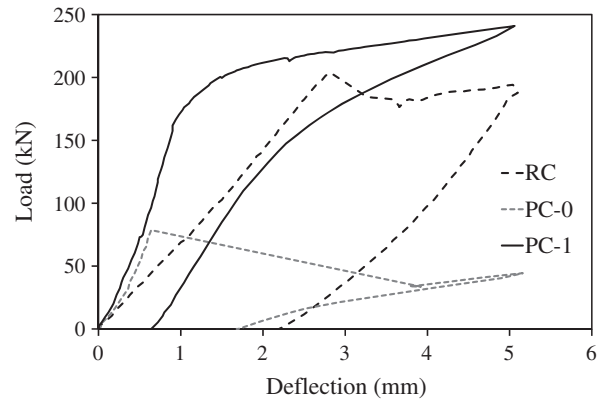
In the RC specimen, the sudden load decrease at approximately 200 kN is attributed to the yielding of the reinforcements. Specimen PC-0 embedding tendons which are not post-tensioned broke under a 78.6 kN load. At this time, the crack width at the joint was larger than 2 mm, and quite visible. The load–deflection response of PC-1 was linear in the range 0–170 kN, but nonlinear outside of this range.

Fig. 12(b) plots the strains on the upper surfaces of the concretes. The residual compressive strain on the PC-0 surface exceeded 500 micro-strain, but was negligible on the RC and PC-1 surfaces. Notably, the load–strain response of PC-1 was nonlinear, consistent with the load–deflection response.

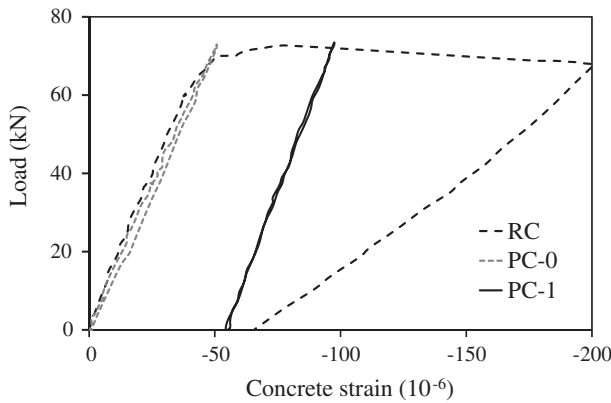
Fig. 12(c) presents the force variation in the prestressing tendons, measured by the load cells. The prestressing tendon forces scarcely changed in the range 0–170 kN, but gradually increased at higher loads. The increased prestressing force may result from



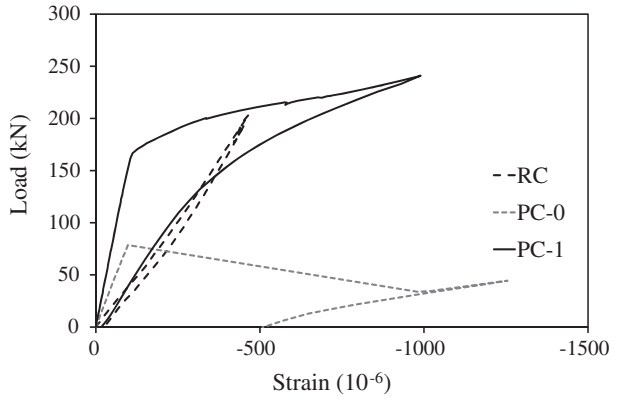
(a) Load versus crack width



(a) Load–deflection responses



(b) Load–strain responses



(b) Load–strain responses

**Fig. 11.** First-phase test results: Load responses of (a) Load versus crack width; (b) Load–strain responses.

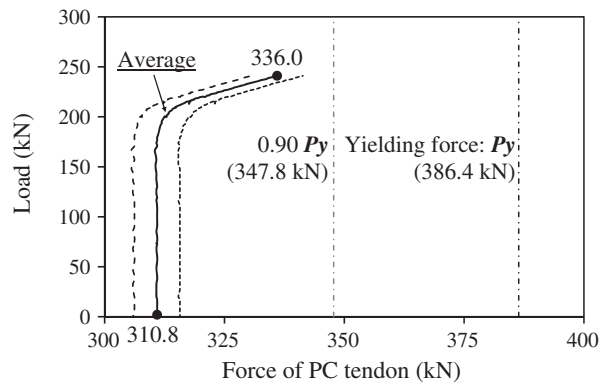
the significantly widened cracks in the joints as the load increases. Note that the increase in the prestressing force (336.0 kN) associated with crack-opening was approximately 13% lower than the yielding force of the tendons (386.4 kN), and is also considerably lower than the pull-out load bearing capacity of 490 kN [17]. This reconfirms that the prestressing tendon is firmly anchored, even under flexural deformation.

### 4.3. Saltwater permeability at the joint

To compare the saltwater permeability at the joints of the concrete specimens, the chloride penetration depths in core extracts were examined by the silver nitrate spraying method. Fig. 13 presents the test results. The average penetration depths of PC-0 and PC-1 were 12.9 mm and 4.2 mm respectively, versus 185.3 mm in the RC specimen. In other words, the penetration depths of PC-0 and PC-1 were 7.0% and 2.3% that of RC, respectively. This observation confirms that the jointed concrete members embedding the tendons are highly impermeable to saltwater. The developed strengthening system with its internal anchorage improves the durability of joints between the existing and new concretes, which are generally vulnerable to steel corrosion.

## 5. Conclusions

This study examined the workability of the developed post-tensioning system in full-size concrete members, and confirmed its improvements to the structural performance and durability of



(c) Forces in the prestressing tendons of PC-1

**Fig. 12.** Third-phase test results: (a) Load–deflection responses; (b) Load–strain responses; (c) Forces in the prestressing tendons of PC-1.

those members in a series of tests. The conclusions of the investigation are summarized below:

- The developed strengthening system significantly reduced the crack widths at the joints between old and new concretes, and improved the load-bearing capacity of the jointed concrete beams.

**Table 6**  
Load bearing capacities and deflections observed in the third phase.

	RC	PC-0	PC-1
Max. deflection $D_{max}$ (mm)	5.10	5.16	5.06
Load at $D_{max}$ (kN)	187.8	44.4	241.0
Load bearing capacity (kN)	203.8	78.6	241.0

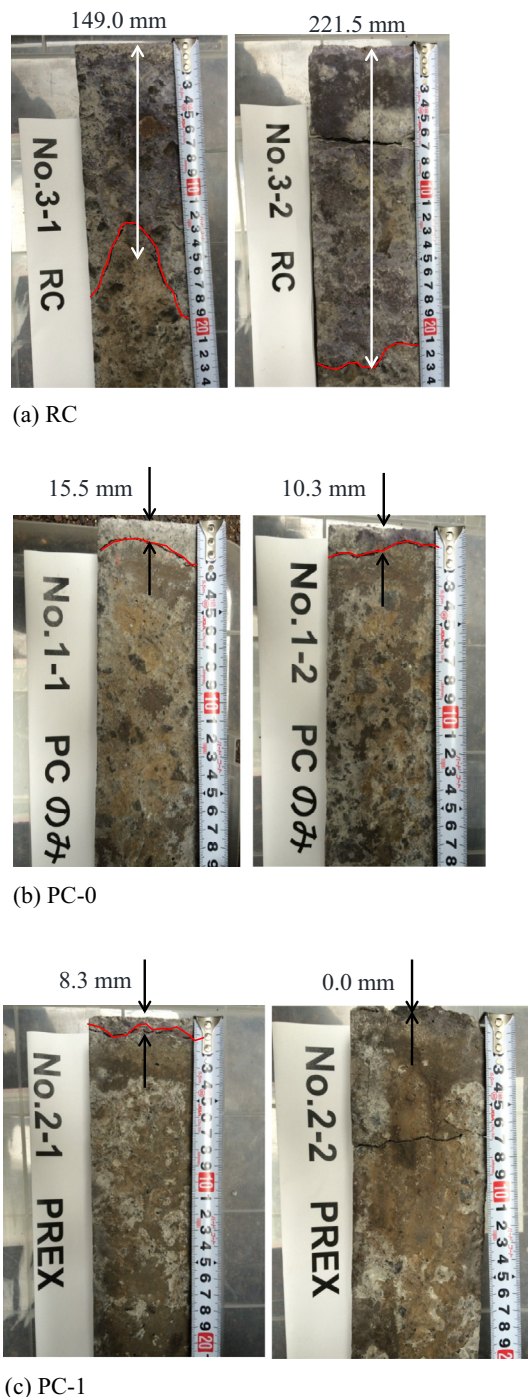


**Fig. 13.** Fourth-phase test results, showing the saltwater permeabilities in the sample cores (a) RC; (b) PC-0; (c) PC-1.

- The force increase in the joints under high load was sufficiently lower than the pull-out capacity in the previous investigation, confirming that the prestressing tendons were firmly anchored even under flexural deformation.
- The jointed concrete member strengthened by the internal prestressing system was significantly less permeable to saltwater than the conventional adhesive anchor system.

This study focused on the applicability and performances of jointed concrete members strengthened by the developed system. For practical applications, experimental and analytical studies of

the structural performance are highly desired, and the effects of the environmental conditions must also be determined.

## Acknowledgments

The authors thank to Dr. Era (Kyokuto Kowa, Co.), Dr. Kawakane (Kyokuto Kowa, Co.), and a graduate student Mr. Mizushima (Yamaguchi University) for their assistance.

## References

- [1] Akiyama M, Abe S, Aoki N, Suzuki M. Flexural test of precast high-strength reinforced concrete pile prestressed with unbonded bars arranged at the center of the cross-section. *Eng Struct* 2012;34:259–70. <http://dx.doi.org/10.1016/j.engstruct.2011.09.007>. Elsevier.
- [2] Clément T, Ramos AP, Ruiza MF, Muttoni A. Influence of prestressing on the punching strength of post-tensioned slabs. *Eng Struct* 2014;72:56–69. <http://dx.doi.org/10.1016/j.engstruct.2014.04.034>. Elsevier.
- [3] El-Hacha R, Wight RG, Green MF. Prestressed fiber-reinforced polymer laminates for strengthening structures. *Progr Struct Eng Mater* 2001;3(2):111–21. <http://dx.doi.org/10.1002/pse.76>. Wiley.
- [4] El-Hacha R, Soudki K. Prestressed near-surface mounted fibre reinforced polymer reinforcement for concrete structures – a review. *Can J Civ Eng* 2013;40(11):1127–39. <http://dx.doi.org/10.1139/cjce-2013-0063>.
- [5] Faria DMV, Lúcio VJG, Ramos AP. Post-punching behaviour of flat slabs strengthened with a new technique using post-tensioning. *Eng Struct* 2012;40:383–97. <http://dx.doi.org/10.1016/j.engstruct.2012.03.014>. Elsevier.
- [6] Faria DMV, Lúcio VJG, Ramos AP. Strengthening of flat slabs with post-tensioning using anchorages by bonding. *Eng Struct* 2011;33:2025–43. <http://dx.doi.org/10.1016/j.engstruct.2011.02.039>. Elsevier.
- [7] Han SW, Kee S-H, Park Y-M, Lee L-H, Kang TH-K. Hysteretic behavior of exterior post-tensioned flat plate connections. *Eng Struct* 2006;28(14):1983–96. <http://dx.doi.org/10.1016/j.engstruct.2006.03.02>. Elsevier.
- [8] Hassanli R, ElGawady MA, Mills JE. Force–displacement behavior of unbonded post-tensioned concrete walls. *Eng Struct* 2016;106:495–505. <http://dx.doi.org/10.1016/j.engstruct.2015.10.035>. Elsevier.
- [9] Japan Concrete Institute (JCI). Practical guideline for investigation, repair and strengthening of cracked concrete structures; 2013 [in Japanese].
- [10] Japan Industrial Standard. Steel bars for prestressed concrete (JIS G 3109); 2008 [in Japanese].
- [11] Kim YJ, Green MF, Wight RG. Effect of prestress levels in prestressed CFRP laminates for strengthening prestressed concrete beams: a numerical parametric study. *PCI J, Prestr Concr Inst (PCI)* 2010;55(2):96–108.
- [12] Kim YJ, Hyun SW, Kang J-Y, Park J-S. Anchorage configuration for post-tensioned NSM CFRP upgrading constructed bridge girders. *Eng Struct* 2014;79:256–66. <http://dx.doi.org/10.1016/j.engstruct.2014.08.022>. Elsevier.
- [13] Koppitz R, Kenel A, Keller T. Punching shear strengthening of flat slabs using prestressed carbon fiber-reinforced polymer straps. *Eng Struct* 2014;76:283–94. <http://dx.doi.org/10.1016/j.engstruct.2014.07.017>. Elsevier.
- [14] Mazaheripour H, Barros JAO, Soltanzadeh F, Sena-Cruz J. Deflection and cracking behavior of SFRSCC beams reinforced with hybrid prestressed GFRP and steel reinforcements. *Eng Struct* 2016;125:546–65. <http://dx.doi.org/10.1016/j.engstruct.2016.07.026>. Elsevier.
- [15] Michels J, Sena-Cruz J, Czaderski C, Motavalli M. Structural strengthening with prestressed CFRP strips with gradient anchorage. *J Compos Constr* 2013;17(5):651–61. [http://dx.doi.org/10.1061/\(ASCE\)CC.1943-5614.0000372](http://dx.doi.org/10.1061/(ASCE)CC.1943-5614.0000372). ASCE.
- [16] Michels J, Martinelli E, Czaderski C, Motavalli M. Prestressed CFRP strips with gradient anchorage for structural concrete retrofitting: experiments and numerical modeling. *Polymers* 2014;6(1):114–31. <http://dx.doi.org/10.3390/polym6010114>. MDPI.
- [17] Mimoto T, Sakaki T, Mihara T, Yoshitake I. Strengthening system using post-tension tendon with an internal anchorage of concrete members. *Eng Struct* 2016;124:29–35. <http://dx.doi.org/10.1016/j.engstruct.2016.06.003>. Elsevier.
- [18] Ng CK, Tan KH. Flexural behaviour of externally prestressed beams. Part I: Analytical model. *Eng Struct* 2006;28:609–21. <http://dx.doi.org/10.1016/j.engstruct.2005.09.015>. Elsevier.
- [19] Ng CK, Tan KH. Flexural behaviour of externally prestressed beams. Part II: Experimental investigation. *Eng Struct* 2006;28:622–33. <http://dx.doi.org/10.1016/j.engstruct.2005.09.016>. Elsevier.
- [20] Turmo J, Ramos G, Aparicio AC. FEM modelling of unbonded post-tensioned segmental beams with dry joints. *Eng Struct* 2006;28(13):1852–63. <http://dx.doi.org/10.1016/j.engstruct.2006.03.028>. Elsevier.
- [21] Park H, Jeong S, Lee S-C, Cho J-Y. Flexural behavior of post-tensioned prestressed concrete girders with high-strength strands. *Eng Struct* 2016;112:90–9. <http://dx.doi.org/10.1016/j.engstruct.2016.01.004>. Elsevier.
- [22] Peng H, Zhang J, Shang S, Liu Y, Cai CS. Experimental study of flexural fatigue performance of reinforced concrete beams strengthened with prestressed CFRP plates. *Eng Struct* 2016;127:62–72. <http://dx.doi.org/10.1016/j.engstruct.2016.08.026>. Elsevier.
- [23] Pillai RG, Hueste MD, Gardoni P, Trejo D, Reinschmidt KF. Time-variant service reliability of post-tensioned, segmental, concrete bridges exposed to corrosive environments. *Eng Struct* 2010;32:2596–605. <http://dx.doi.org/10.1016/j.engstruct.2010.04.032>. Elsevier.

- [24] Schmidt JW, Bennitz A, Taljsten B, Goltermann P, Pedersen P. Mechanical anchorage of FRP tendons – a literature review. *Constr Build Mater* 2012;32:110–21. <http://dx.doi.org/10.1016/j.conbuildmat.2011.11.049>. Elsevier.
- [25] Vu NA, Castel A, François R. Response of post-tensioned concrete beams with unbonded tendons including serviceability and ultimate state. *Eng Struct* 2010;32(2):556–69. <http://dx.doi.org/10.1016/j.engstruct.2009.11.001>. Elsevier.
- [26] Yang K-H, Mun J-H, Kim G-H. Flexural behavior of post-tensioned normal-strength lightweight concrete one-way slabs. *Eng Struct* 2013;56:1295–307. <http://dx.doi.org/10.1016/j.engstruct.2013.07.00>. Elsevier.
- [27] You Y, Choi K, Kim J. An experimental investigation on flexural behavior of RC beams strengthened with prestressed CFRP strips using a durable anchorage system. *Compos: Part B* 2012;43:3026–36. <http://dx.doi.org/10.1016/j.compositesb.2012.05.030>. Elsevier.
- [28] Wang X, Shi J, Wu G, Yang L, Wu Z. Effectiveness of basalt FRP tendons for strengthening of RC beams through the external prestressing technique. *Eng Struct* 2015;101:34–44. <http://dx.doi.org/10.1016/j.engstruct.2015.06.052>. Elsevier.
- [29] Aaleti A, Sritharan S. A simplified analysis method for characterizing unbonded post-tensioned precast wall systems. *Eng Struct* 2009;31(12):2966–75. <http://dx.doi.org/10.1016/j.engstruct.2009.07.024>.